

## ARTICLE OPEN



# Taraxasterol prompted the anti-tumor effect in mice burden hepatocellular carcinoma by regulating T lymphocytes

Feng Ren<sup>1,2,6</sup>, Yu Zhang<sup>1,2,6</sup>, Yuanhua Qin<sup>1,2</sup>, Jingli Shang<sup>1,2</sup>, Yanling Wang<sup>1,2,3,4</sup>, Pengkun Wei<sup>1,2,3,5</sup>, Jiaming Guo<sup>1,3</sup>, Huijie Jia<sup>1,3,4</sup> and Tiesuo Zhao<sup>1,3,5</sup>

© The Author(s) 2022

Hepatocellular carcinoma (HCC) is a common digestive malignant tumor with high morbidity and mortality worldwide, however, the treatment of HCC and prognosis of patients are not optimistic, finding more effective treatments are imperative. *Taraxacum officinale* (L.) Weber ex F.H.Wigg is a perennial herb of compositae, and our study has demonstrated that *Taraxacum officinale* polysaccharide has certain anti-tumor effect on HCC cells. Taraxasterol (TS) is a natural product extracted from *Taraxacum officinale* with strong physiological, pharmacological and biological activities, but the effect of TS on HCC is yet to be determined. Therefore, the aim of this study is to explore the effect of dandelion sterol on HCC in vivo and in vitro. The results showed that TS significantly inhibited the proliferation, induced apoptosis and blocked cell cycle in HCC cell lines HepG2 and Huh7 cells in vitro. TS inhibited the tumor growth of H22 bearing mice and the expression of Ki67 in vivo. More importantly, TS regulated the immunity of H22 bearing mice by elevating the ratio of CD4<sup>+</sup> T cells in spleen, and increasing the number of T cell infiltration in tumor tissue. Except immunomodulation, the mechanism of tumor growth inhibition may be related to the regulation of apoptosis related proteins and IL-6/STAT3 pathway. TS significantly inhibited the growth of HCC cells both in vitro and in vivo. The study would provide a theoretical basis for the new application of TS and the adjuvant treatment of malignant tumor with traditional Chinese medicine.

*Cell Death Discovery* (2022)8:264; <https://doi.org/10.1038/s41420-022-01059-5>

## INTRODUCTION

As a highly common malignant tumor of digestive tract, hepatocellular carcinoma ranks second of cancer deaths in the world in 2020. Even with the continuous progress of various treatment methods, the 5-year survival rate of liver cancer is only 20% [1]. Therefore, the research on the treatment of hepatocellular carcinoma has always been concerned.

*Taraxacum officinale* (L.) Weber ex F.H.Wigg has long been traditionally used as a kind of Chinese herbal medicine for disorders of the liver, breast and gallbladder as well as hepatitis and digestive diseases [2–6]. However, the components of *Taraxacum officinale* are complex, so it is very important to find the specific components of *Taraxacum officinale*. Taraxasterol (TS) is a natural product extracted from *Taraxacum officinale* with strong physiological [7], pharmacological and biological activities [8]. Researches have demonstrated that it has anti-inflammation, anti-cancer and other pharmacological activities, while the effect of TS on proliferation of the HCC cells is yet to be determined. It is easily available, wide occurrence in plants, stable properties and anti-tumor activity, making it an attractive target for drug development. Although some studies have shown that TS delayed the progression of mice with rheumatoid arthritis by inhibiting inflammatory response [7], however, its anti-tumor immune response is not clear.

Along with advances in immunology, more and more attention has been paid to the role of anti-liver cancer by regulating the immune system [9]. As we all know, the body's immune system is suppressed in the patients with liver cancer, which leads to immune escape of tumor cells and accelerates tumor progression. Indeed, several preclinical and clinical data support this hypothesis showing that immunotherapy and even more their combination may be a good alternative candidate for the treatment of HCC patients [10, 11]. As a very important adaptive immune cell, T lymphocytes play a very important role in anti-tumor. Studies have shown that the number of T cell infiltration in tumor tissue is closely related to the prognosis of patients [12, 13]. Therefore, T cell-associated immunotherapy lights up the hope for the improvement of complementary approach to conventional HCC treatments. So far, many traditional Chinese medicines have been proved to have certain role in regulating immune function [14, 15]. *Taraxacum officinale* polysaccharide can be developed as a new immune enhancer because of its good immune regulation ability [16]. However, its effect on T cells needs to be further studied. In particular, the effect of sterol, a specific component of polysaccharide, on T cells is also not clear.

Therefore, in this study, the effect of TS on the proliferation of HCC cells was explored in vivo and in vitro, and its regulatory effect on T cells was further clarified. The study would provide a

<sup>1</sup>Basic Medical College, Xinxiang Medical University, Xinxiang 453000 Henan, PR China. <sup>2</sup>Henan International Joint Laboratory of Immunity and Targeted Therapy for Liver-Intestinal Tumors, Xinxiang Medical University, Xinxiang 453000 Henan, PR China. <sup>3</sup>Xinxiang Key Laboratory of Tumor Vaccine and Immunotherapy, Xinxiang Medical University, Xinxiang 453000 Henan, PR China. <sup>4</sup>Department of Pathology, Xinxiang Medical University, Xinxiang 453000 Henan, PR China. <sup>5</sup>Department of Immunology, Xinxiang Medical University, Xinxiang 453000 Henan, PR China. <sup>6</sup>These authors contributed equally: Feng Ren, Yu Zhang. ✉email: zhongziqu1115@163.com; 131009@xxmu.edu.cn

Received: 17 January 2022 Revised: 22 April 2022 Accepted: 5 May 2022

Published online: 16 May 2022

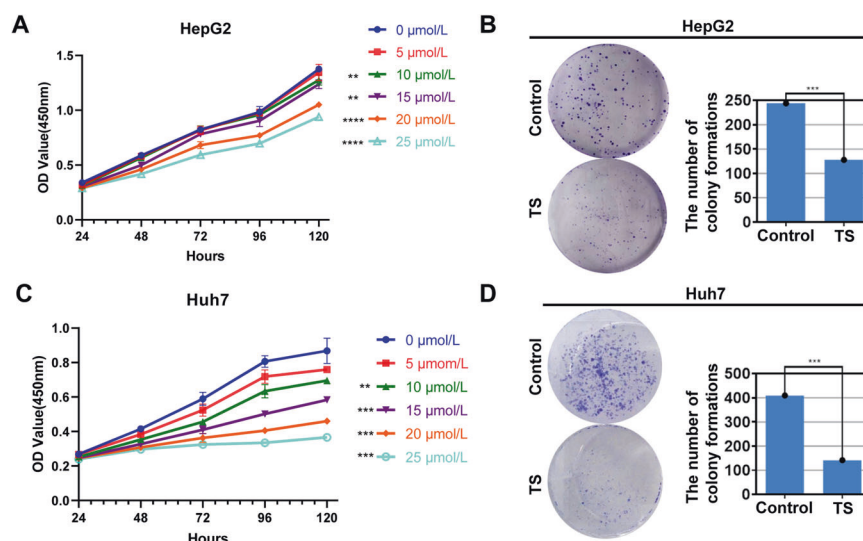


**Fig. 1** TS significantly inhibited the proliferation of hepatoma cells in vitro. **A** The effect of different concentrations of TS (0, 5, 10, 15, 20 and 25  $\mu\text{mol/L}$ ) on the viability of HepG2 during 24 to 120 h via CCK-8. **B** The effect of TS (15  $\mu\text{mol/L}$ ) on colony forming ability of HepG2 measured by cell clone formation experiment. **C** The effect of TS with different concentrations of 0, 5, 10, 15, 20 and 25  $\mu\text{mol/L}$  on the viability of Huh7 from 24 to 120 h through CCK-8. **D** The effect of TS (15  $\mu\text{mol/L}$ ) on colony forming ability of Huh7 detected by cell clone formation experiment. Results were obtained from experiments carried out in triplicate from at least three independent experiments. Data are presented as the mean  $\pm$  SD ( $n = 5$ ). \* $p < 0.05$  vs. the Control group; \*\* $p < 0.01$  vs. the Control group; \*\*\* $p < 0.001$  vs. the Control group.

theoretical basis for the new application of TS and the development of *Taraxacum officinale* resources.

## RESULTS

### TS significantly inhibited the proliferation of hepatoma cells

Firstly, we detected the effects of the TS at different concentrations (5, 10, 15, 20 and 25  $\mu\text{mol/L}$ ) on the growth of two hepatoma cell lines HepG2 and Huh7. The results showed that when concentration was 10 and 15  $\mu\text{mol/L}$ , TS suppressed the proliferation of HepG2 cells only at 120 h, while when the concentration was more than 20  $\mu\text{mol/L}$ , it markedly inhibited the proliferation of HepG2 cells at 48, 72, 96 and 120 h (Fig. 1A). The results of cell cloning experiment are consistent with the above results (Fig. 1B). In addition, the TS also inhibited the proliferation of Huh7 cells at 72, 96 and 120 h when the concentration was more than 5  $\mu\text{mol/L}$ , while when the concentration reached 10  $\mu\text{mol/L}$ , it extremely inhibited the proliferation of Huh7 cells for more than 48 h incubation (Fig. 1C). The cell cloning experiment shows similar results (Fig. 1D).

### Effects of TS on apoptosis and cell cycle of HepG2 and Huh7 cells

In order to detect the effect of TS on cell apoptosis and cell cycle of HepG2 and/or Huh7 cells, the Annexin V-FITC-PI apoptosis double staining and the cell cycle changes were performed by flow cytometry. The results demonstrated that the apoptosis rate of HepG2 hepatoma cells in the control group was 6.48%, however, after treatment with TS (15  $\mu\text{mol/L}$ ) for 72 h, the apoptosis rate of HepG2 increased to 9.095% (Fig. 2A); while the apoptosis rate of Huh7 hepatoma cells in the control group was 14.17%, and after treatment with TS (15  $\mu\text{mol/L}$ ) for 72 h, the apoptosis rate of Huh7 hepatoma cells increased to 23.4% (Fig. 2B). The results indicated that TS could induce apoptosis of human hepatoma cells. Moreover, the results from cell cycle showed that compared with the control group, the proportion of cells in G1 phase was increased after treat with TS, while that in G2 phase decreased was in TS group (Fig. 2C). Besides, the expression of cell cycle relative protein Cyclin D1 was also detected using WB assay, and the results showed that TS with the

concentration of 15  $\mu\text{mol/L}$  also markedly suppressed the expression of Cyclin D1 as compared with that in the control group (Fig. 2D, E), indicating that treatment with TS could induce G1 phase arrest of HepG2 cells.

### Effect of TS on tumor growth of tumor bearing mice

Next, we examined the effect of TS on tumor growth of H22 hepatoma-bearing mice. The results showed that TS at the doses of 5 and 7.5 mg/kg notably suppressed the tumor growth of the tumor bearing mice (Fig. 3A–C). As shown in Fig. 3D–F, the expression of apoptosis related protein cleaved caspase-3 was significantly elevated while the apoptotic cells in tumor tissues were markedly reduced after treatment with TS at the concentration of 5 or 7.5 mg/kg, which is similar to the results in vitro. Moreover, cell proliferation was measured by staining for the proliferation markers Ki-67. Immunohistochemistry for Ki-67 illustrated inhibited staining of proliferate uncials in tumor tissues after treated by TS (Fig. 3G), indicating that TS can effectively inhibit the proliferation of tumor cells.

### Effect of TS on the ratio of T cells in spleen and T cell infiltration in tumor tissue of hepatoma-bearing mice

Many studies have shown that traditional Chinese medicine could improve the immune response. So, we next investigated the ratio of T cells in the spleen of tumor bearing mice. The results showed that TS significantly increased the ratio of  $\text{CD4}^+$  T cells in the spleen after treatment with a dose of 7.5 mg/kg (Fig. 4A, B), but had no significant effect on the ratio of  $\text{CD8}^+$  T cells (Fig. 4C, D). We further examined the effect of TS on T cell infiltration in tumor tissues of hepatoma-bearing mice. The results showed that TS with the dosage of 5 mg/kg not only increased the infiltration of  $\text{CD4}^+$  T cells in tumor tissue (Fig. 4E), but also increased the infiltration of  $\text{CD8}^+$  T cells (Fig. 4F), which is more obvious in 7.5 mg/kg group.

### Effect of TS on the expression of apoptosis related proteins and IL-6/STAT3 pathway related proteins in HCC cells

In order to explore other mechanism related to the tumor inhibition by TS. We further detected several proteins expression

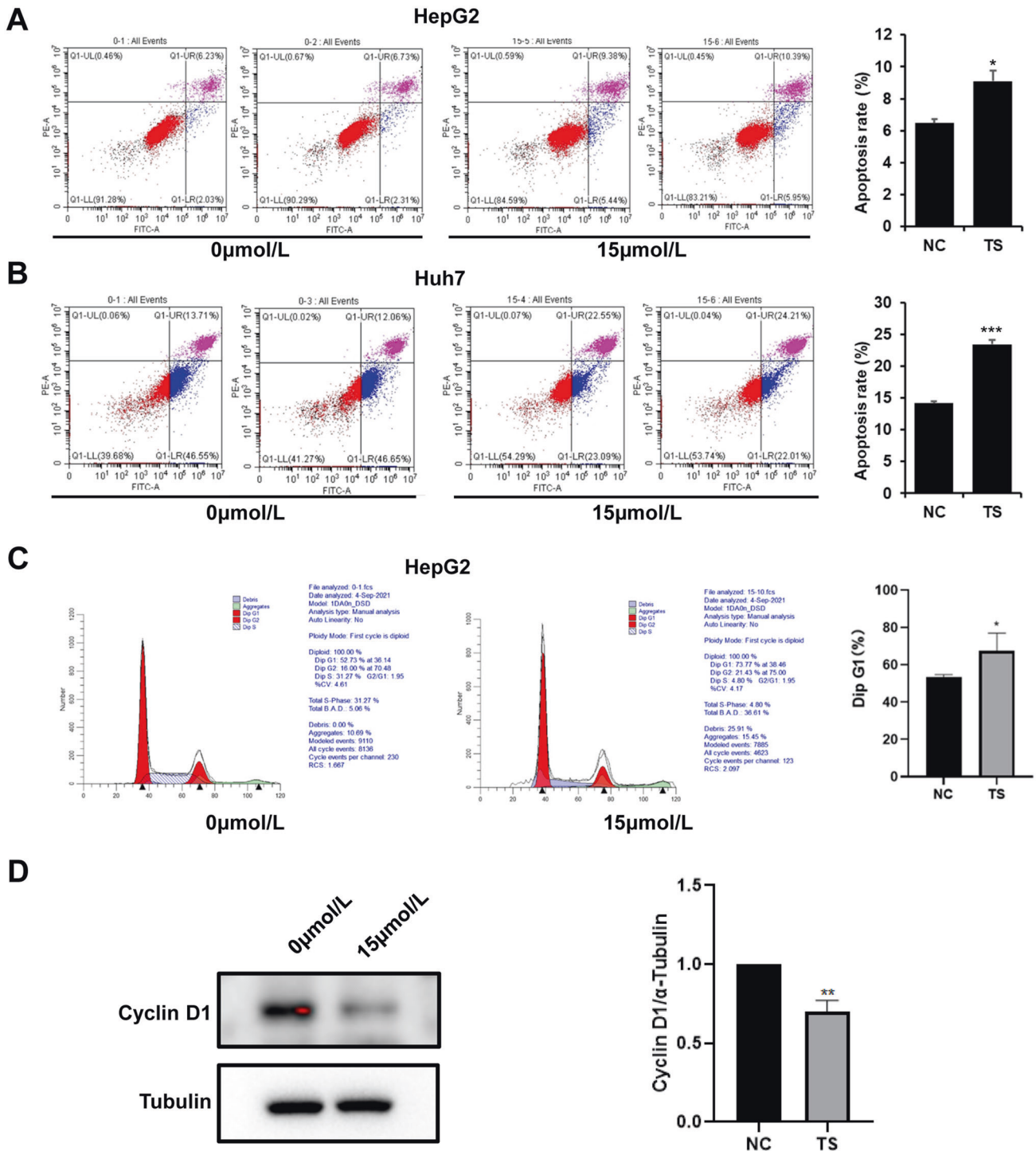


**Fig. 2** TS induced apoptosis and blocked cell cycle of hepatoma cells in vitro. The effect of TS with 15 μmol/L on apoptotic rate of HepG2 (A) and Huh7 (B) after 72 h using annexin V/PI double staining. C The effects of TS with 15 μmol/L on the cell cycle of HepG2 through propidium iodide staining. D The expression of Cyclin D1 after treated with TS by WB assay and the statistical analysis. Results were obtained from experiments carried out in triplicate from at least three independent experiments. Data are presented as the mean ± SD ( $n = 5$ ). \* $p < 0.05$  vs. the Control group; \*\* $p < 0.01$  vs. the Control group; \*\*\* $p < 0.001$  vs. the Control group.

using WB. The results showed that the translation of both oncogene STAT3 and its upstream gene IL-6 were downregulated after TS treatment (Fig. 5A, B). Additionally, the apoptotic protein marker Bcl-2 was inhibited while cleaved caspase-3 was increased (Fig. 5C, D). These results indicated that TS affected the expression of apoptosis related proteins and IL-6/STAT3 pathway related proteins in HCC related cell lines.

## DISCUSSION

Hepatocellular carcinoma is the most common primary malignancy of the liver in adults and the main cause of cancer-related death worldwide with few efficacious therapeutic options for this deadly disease [17]. This study explored the therapeutic effect of TS on hepatocellular carcinoma. The results showed that TS is capable of inhibiting tumor cell proliferation, inhibiting the growth

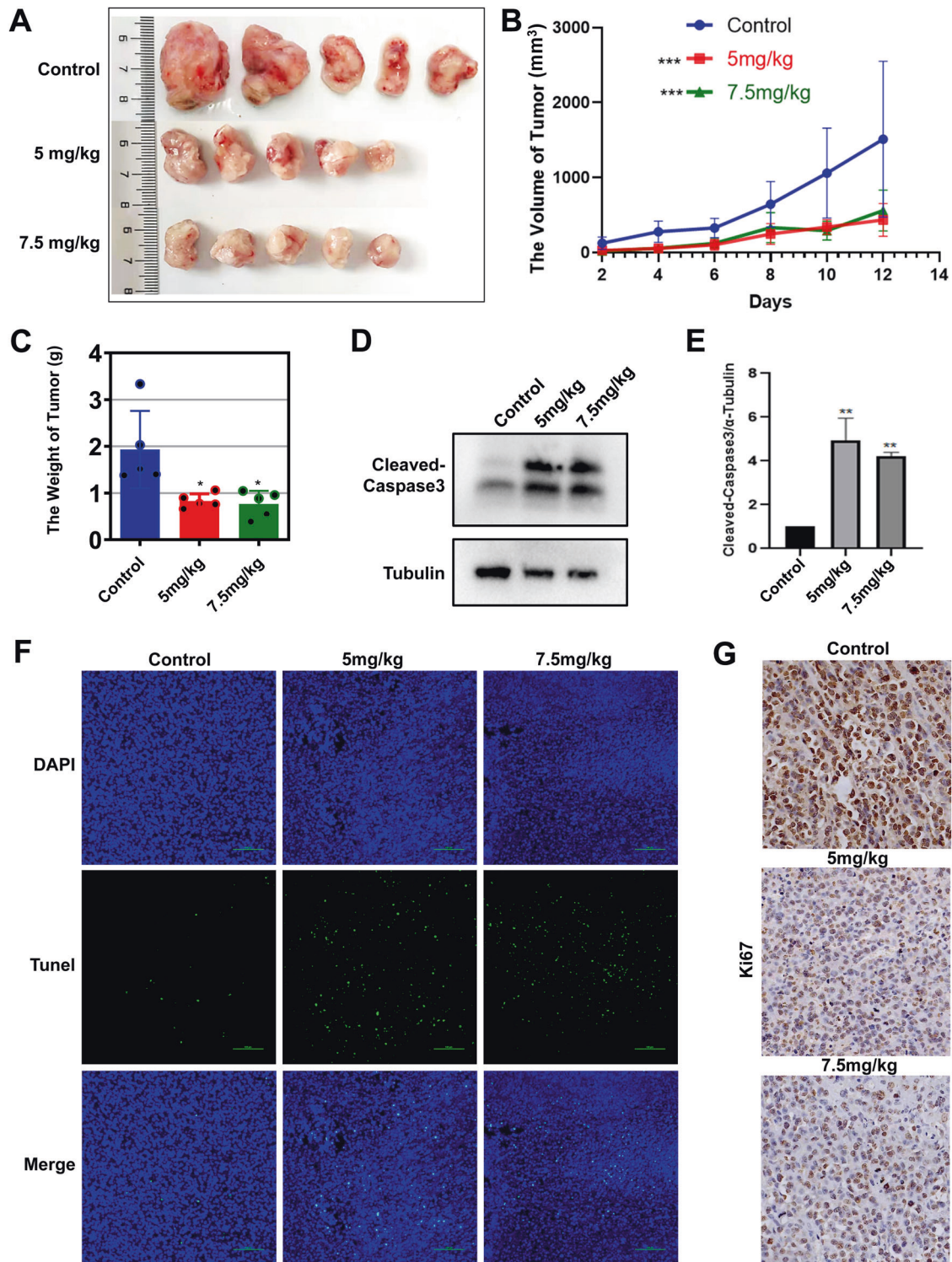


**Fig. 3** TS inhibited tumor growth of H22 tumor bearing mice in vivo. **A** The image of tumor from H22 tumor bearing mice. **B** Tumor weight of H22 tumor bearing mice. **C** Tumor volume changes of H22 tumor bearing mice. **D** The expression of cleaved Caspase-3 after treated with TS by WB assay in vivo. **E** The statistical analysis for the WB assay in **D**. **F** The apoptotic cells in tumor tissue after treatment with TUNEL. **G** Ki-67 immunohistochemistry of the tumor sections in H22 tumor bearing mice (40×). Results are from independent duplicate or triplicate experiments and presented as means ± SD. Number of mice per group are seven ( $n = 5$ ). \* $p < 0.05$  vs. the Control group; \*\* $p < 0.01$  vs. the Control group; \*\*\* $p < 0.001$  vs. the Control group.

of tumor and improving the anti-tumor immunity of tumor bearing mice.

Cancer progression is known to involve the degree of proliferation. Taraxacum officinale root extract (TRE) has

demonstrated therapeutic anti-tumor activity in different cancer cell models. It was showed that as TRE potently inhibited proliferation and migration and expedited apoptosis in gastric carcinoma cells [18]. Another study illustrated that TRE affected

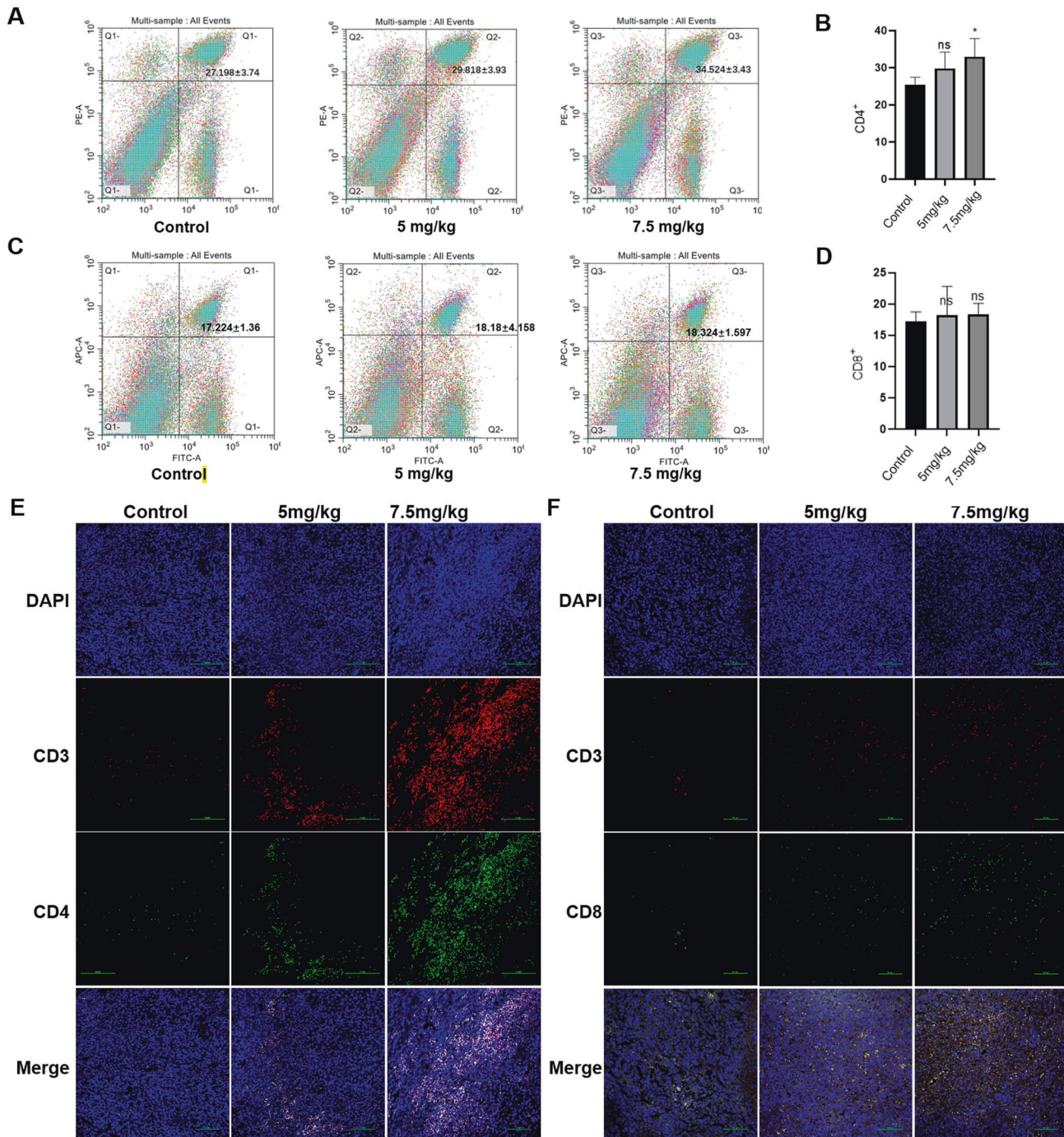


**Fig. 4** TS promoted the immune regulation of H22 tumor bearing mice. **A** The proportion of CD4<sup>+</sup> T cells in the spleen of tumor bearing mice were detected by flow cytometry. **B** The analysis of the results from **A**. **C** The proportion of CD8<sup>+</sup> T cells in the spleen of tumor bearing mice were detected by flow cytometry. **D** The analysis of the results from **C**. The infiltration of CD4<sup>+</sup> (**E**) /CD8<sup>+</sup> (**F**) T cells in tumor tissue sections were detected by immunofluorescence (20×). Results are from independent duplicate or triplicate experiments and presented as means ± SD. Number of mice per group are seven ( $n = 7$ ). \* $p < 0.05$  vs. the Control group; \*\* $p < 0.01$  vs. the Control group; \*\*\* $p < 0.001$  vs. the Control group.

the proliferation by activating a multiplicity of death signaling pathways in colorectal cancer without toxicity to non-cancerous cells [19].

Our previous studies also found that DP inhibited the proliferation of HCC in vitro and in vivo [20]. In order to further clarify the role of specific components in TS, we detected the effect of TS on the proliferation of HCC cells. The results showed that it significantly inhibited the proliferation of HCC cells, which

was related to the fact that sterols could inhibit the cell cycle of tumor cells. Cell proliferation specific antigen Ki67 is an important protein for the detection of cell proliferation activity [21, 22], which is often detected by immunohistochemistry. Besides, proliferating cell nuclear antigen and micro chromosome maintenance proteins are also the basic proliferation markers commonly used to evaluate the growth fraction of cell populations [23]. Our results illustrated that TS effectively inhibited HCC

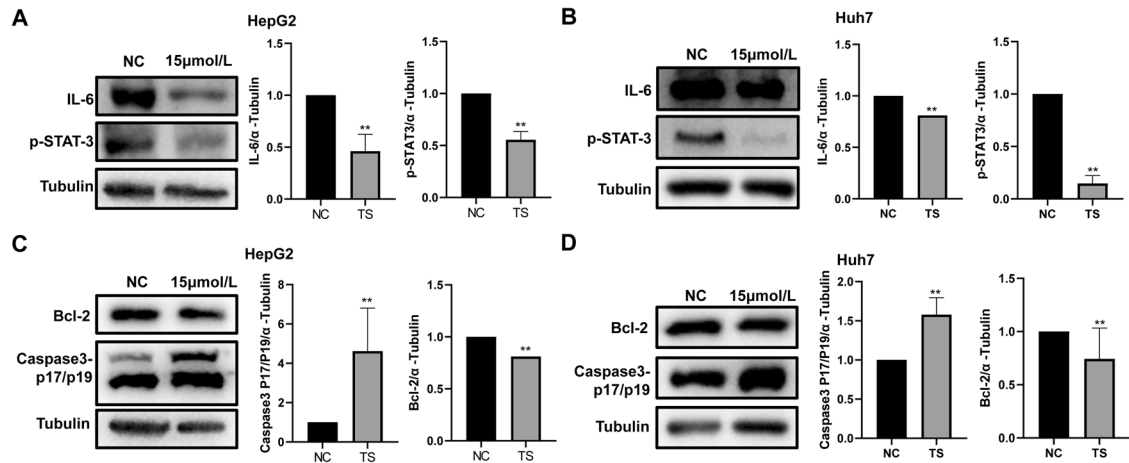


**Fig. 5** TS affected the expression of apoptosis related proteins and IL-6/STAT3 pathway related proteins in HepG2 and Huh7 cells. The expression of IL-6 and p-STAT-3 after treatment by TS (15  $\mu\text{mol/l}$ ) in HepG2 cells (A) and Huh7 cells (B). The expression of apoptosis related proteins (Bcl-2 and cleaved Caspase-3) after treatment by TS in HepG2 cells (C) and Huh7 cells (D). Results were obtained from experiments carried out in triplicate from at least three independent experiments. Data are presented as the mean  $\pm$  SD ( $n = 5$ ). \* $p < 0.05$  vs. the Control group; \*\* $p < 0.01$  vs. the Control group; \*\*\* $p < 0.001$  vs. the Control group.

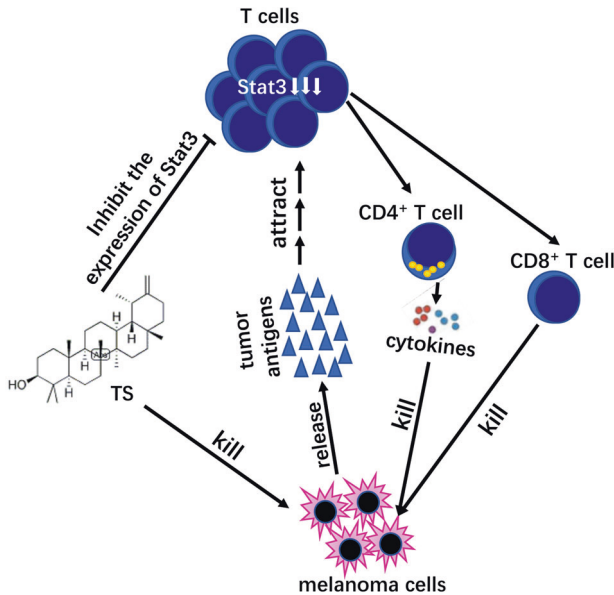


**Fig. 6** Hypothesis of the mechanism about TS anti HCC. The high expression of STAT3 will not only significantly promote tumor progression, but also mediate tumor immune escape, and the results further confirmed that TS could significantly inhibit the expression of STAT3 protein in tumor tissues. Therefore, we hypothesizes that the anti-tumor mechanism of TS is as follows: firstly, TS causes the apoptosis of tumor cells, which would enable tumor cells to release more tumor antigens, chemotactic a large number of  $\text{CD4}^+$  and  $\text{CD8}^+$  T lymphocytes to reach tumor tissues and play an anti-tumor role. In addition, TS could inhibit the expression of STAT3 protein in T cells and further enhance the anti-tumor effect of T cells, and finally improve the anti-tumor immune response of tumor bearing mice.

cell proliferation by inhibiting the expression of Ki67. These results provide experimental evidence for the development of anti-tumor drugs based on *Taraxacum officinale* extract.

At present, HCC has been considered an immunogenic tumor [24]. Therefore, immunotherapeutic approaches might be a more appropriate therapeutic strategy. It was confirmed that immune response and hepatocellular carcinoma progression are closely related. The role of the immune system in the control of cancer

initiation and progression has been demonstrated in recent decades [25]. It was found that the anti-tumor immune response was inhibited in hepatocellular carcinoma patients, leading to immune escape. T lymphocyte, as an important immune cell, is highly important in immune response and anti-tumor response [26].

The traditional medicine has been used for years in treatment of cancer patients. It may not only attenuate the severity of tumor symptoms and improve the quality of life, but also control the size of tumor and prolong the survival of patients. It is known that many traditional Chinese medicines inhibit tumor growth by affecting the immune system [27]. Some traditional Chinese medicines serve an anti-tumor role in immunosuppressive tumor microenvironment through upregulating immune response [28]. Tumor-infiltrating lymphocytes, which can recognize tumor cells and provoke an anti-tumor response plays an active role in the survival of patients with hepatocellular carcinoma [29]. There are also reports the ratios of tumor-infiltrating  $\text{CD4}^+/\text{CD8}^+$  are associated with the survival of the patients with HCC [30]. As effector cytotoxic T lymphocytes,  $\text{CD8}^+$  T cells can recognize cancer antigens presented by major histocompatibility complex molecules and dissolve tumor cells by releasing granzyme and perforin after activation.  $\text{CD4}^+$  T cells can enhance the function of tumor specific  $\text{CD8}^+$  T cells by secreting interleukin-2, which can effectively promote tumor regression [31]. Our results showed that TS not only effectively increased the ratio of  $\text{CD4}^+$  T cells in the spleen of tumor bearing mice, but also elevated the infiltration of  $\text{CD4}^+$  and  $\text{CD8}^+$  T cells in tumor tissues. It was confirmed that TS played an anti-tumor role by regulating T cells, though this effect is even more pronounced for the regulation of  $\text{CD4}^+$  T cells. The mechanism may be related to the expression of STAT3 (Fig. 6).

## MATERIALS AND METHODS

### Cell Counting Kit-8 analysis

Human HCC cell lines (HepG2 and Huh7) were provided by Stem Cell Bank, Chinese Academy of Sciences. TS was purchased from Chengdu Ruifensi Biotechnology Co., Ltd, China (purity  $\geq 99\%$ , and endotoxin free) [32]. Huh7 or HepG2 cells were prepared into 96-well plates with a density of  $2 \times 10^3$  cells/well and incubated for 14–16 h at  $37^\circ\text{C}$  with the condition of  $5\% \text{CO}_2$ . Then TS with the different concentrations of 0, 5, 10, 15, 20 and  $25 \mu\text{mol/l}$  were added, respectively. After co-cultured for 24, 48, 72, 96 or 120 h, CCK-8 was added to each well and incubated for another 2 h. Finally, the OD value at the wavelength of 450 nm was detected by an enzyme-labeling instrument (Molecular Devices, USA). The changes of cell activity after administration for 24, 48, 72, 96 or 120 h were measured and plotted.

### Cell clone formation experiment

The cells in logarithmic growth stage were seeded into the 6-well plates, with  $8 \times 10^3$  cells/well (Huh7) and  $2 \times 10^3$  cells/well (HepG2). After 24 h, TS was added at concentrations of 0, 5, 10, 15, 20 and 25  $\mu\text{mol/l}$ . The cells were observed every day, and the culture medium was changed every 2 days. When the cells grew into clusters, the culture medium was removed, and each well was washed twice with PBS and sucked out with a pipette. Then, 1 ml 4% (wt/vol) paraformaldehyde was added into each well, which was fixed for 30 min at room temperature and then removed. Subsequently, 1 ml crystal violet was added into each well and stained for 15 min. The 6-well plate was washed with ultrapure water, and then images were captured and saved. The plate was inverted and a piece of transparent film with a grid was superimposed. The number of clones with  $>10$  cells was counted under the microscope (Nikon, Tokyo, Japan). Finally, the clone formation rate was calculated: Clone formation rate = (clones/inoculated cells)  $\times$  100%.

### Establishment of subcutaneous tumor model in mice

Mouse HCC cell line H22 was obtained from China Center for Type Culture Collection. Kunming mice (female, 6–8 weeks) were purchased from Experimental animal center of Xinxiang Medical University. The mice were fed in pathogen-free conditions, housed under a 12 h light/dark cycle at a temperature of  $25 \pm 2^\circ\text{C}$ . H22 cells was inoculated subcutaneously into Kunming mice. Mice were randomly divided into three groups: control group, treatment with 5 mg/kg TS group and treatment with 7.5 mg/kg TS group, with seven mice in each group. When the tumor grew to a sufficient size (about  $100 \text{ mm}^3$ ) for 5–7 days, the mice were given 0.1 ml PBS or different concentrations of TS per day via gavage for 14 days. The tumor volume of mice was measured every other day until it reached to  $1500 \text{ mm}^3$ . The mice were killed, the tumors were removed, weighed, and photographed. Tumors from the mice were fixed overnight and embedded in paraffin. All animal studies were performed according to protocols approved by the Ethics Committee of Xinxiang Medical University.

### Apoptosis analysis

HepG2 and Huh7 cells were cultured and treated with different concentrations of TS (0 and 15  $\mu\text{mol/l}$ ). After 72 h, the cells ( $2 \times 10^6$ ) were collected and mixed with 100  $\mu\text{L}$  Annexin V binding buffer. The cells were added with 5  $\mu\text{L}$  Annexin V-FITC and 5  $\mu\text{L}$  PI Solution for 15 min and then were added with 400  $\mu\text{L}$   $1 \times$  Annexin V Binding Solution. The ratio of apoptosis was analyzed by the flow cytometry (Cytoflex, Beckman).

### Cell cycle detection

HepG2 cells were cultured and treated with different concentrations of TS (0 and 15  $\mu\text{mol/l}$ ) for 72 h. The cells ( $5 \times 10^5 - 1 \times 10^6$ ) were fixed with 75% ethanol at  $4^\circ\text{C}$  overnight. Subsequently, cells were then washed with PBS and labeled with Propidium iodide staining solution and added with RNase A. Cell cycle assays were performed with the flow cytometry (Cytoflex, Beckman) and analyzed with Modfit Software (Topsham, ME).

### Western blot

HepG2 cells and Huh7 cells were treated with TS for 72 h. The protein was then extracted with RIPA lysis buffer (Solarbio life sciences, Beijing, China) and the concentration was determined using a bicinchoninic acid protein assay. For tumor tissue, 0.1 g of tissue were weighed and grinded, 600  $\mu\text{L}$  RIPA lysate was added on ice for 30 min, and then centrifuged (8000r for 10 min) at  $4^\circ\text{C}$ . The supernatant was collected, the loading buffer (Beyotime Institute of Biotechnology, Shanghai, China) was added, and the protein lysis sample was boiled for 13 min at  $95^\circ\text{C}$ . The protein samples were separated by 12 and 8% sodium dodecyl sulfate-polyacrylamide gel electrophoresis and transferred to polyvinylidene fluoride membranes (Millipore, Billerica, MA, USA). The membranes were blocked with 5% non-fat milk for 2 h at room temperature and then incubated with the following primary antibodies of  $\alpha$ -Tubulin (1:1000; Beyotime; AF0001), Caspase-3 P17/P19 (1:1000; Proteintech; 19677-1-AP), Cleaved Caspase-3 (1:1000, CST; 9664), IL-6 (1:1000, Abcam; ab258341), Bcl-2 (1:1000; proteintech; 12789-1-AP), Cyclin D1 (1:1000; Proteintech; 26939-1-AP) and p-STAT-3 (1:1000; CST; 9145) overnight at  $4^\circ\text{C}$ . The membrane was then incubated with Goat Anti-Rabbit IgG antibody (1:3000, Cwbio; CW01035). Specific immune complexes were visualized using enhanced chemiluminescence (Beyotime Institute of Biotechnology) and semi-quantified with the software of multifunctional chemiluminescence imaging system (Viliber, France).

### Immunohistochemistry

Tumor tissues were fixed in 4% formalin for 24 h, embedded in paraffin, and sectioned into 5  $\mu\text{m}$  thick sections. The sections were deparaffinized and dehydrated in a series of xylene and alcohol washes. Then, antigen retrieval was performed by heating the tissue sections in a microwave for 10 min in a citrate solution (10 mmol/l; pH 6.0). The tissues were then blocked with 1% (wt/vol) BSA (Gibco; Thermo Fisher Scientific, Inc.) at room temperature for 15 min and incubated with monoclonal antibodies directed against Ki67 (1:2000; Proteintech Group, Inc., Chicago, IL, USA; 23709-1-AP) overnight at  $4^\circ\text{C}$ . The sections were rinsed with PBS for 5 min and blocked with HRP-conjugated immunoglobulin G secondary antibody (1:1000; ZSGB-BIO, Beijing, China) for 30 min at room temperature. The slices were colored by DAB for 5 min at room temperature, counterstained with hematoxylin for 1 min, differentiated by hydrochloric ethanol, and finally sealed with neutral resin glue, scanned and photographed under light microscope.

### Terminal deoxynucleotidyl transferase (TdT)-mediated dUTP nickend labeling (TUNEL)

Tumor tissues were fixed in 4% formalin for 24 h, embedded in paraffin, and sectioned into 5  $\mu\text{m}$  thick sections. The apoptosis of cells in tumor tissues is detected by TUNEL assay kit (Beyotime Institute of Biotechnology, Shanghai, China) according to the instruction. Firstly, the TUNEL detection solution is dropwise added on the surface of tumor sections and incubated in dark at  $37^\circ\text{C}$  for 60 min. Then the sections are washed using PBS for 10 min and three times. Finally, the sections are dried and sealed with the solution of anti-fluorescence quenching, and observed the image using the fluorescence microscope.

### Flow cytometry

The spleen was isolated under sterile conditions and grounded with ground glass. The suspension is sucked out, filtered with a filter screen (200 mesh, 70UM), and then centrifuged. The erythrocyte lysate was added for 2 min, which was centrifuged and then was adjusted to  $1 \times 10^9/\text{ml}$ . The antibodies CD3/CD4/CD8 were added respectively and incubated on ice in dark for 30 min. In total, 1640 of 200  $\mu\text{L}$  was added to resuspended cells and centrifuged. The supernatant was discarded and the cells were washed with 300  $\mu\text{L}$  precooled PBS. Each sample was filtered with filter trap EP with light avoid. The sample was tested with flow cytometry immediately.

### Immunofluorescence

Tumor tissues were fixed in 4% formalin for 24 h, embedded in paraffin, and sectioned into 5  $\mu\text{m}$  thick sections. The antigen was repaired by microwave and the endogenous catalase activity was eliminated by 3% catalase. The sections were blocked with 10% goat serum and incubated with primary anti mouse anti-CD3 (1:100)/mouse anti-CD4 (1:150)/rabbit anti-CD8 (1:600) at  $4^\circ\text{C}$  overnight. The slices were washed with PBS for three times, and then incubated with fluorescent secondary antibody (1:200) at room temperature for 30 min. The slices were washed three times with PBS and then incubated with DAPI at room temperature for 5 min. The slices were washed with PBS for three times, and then sealed with anti-fluorescence attenuation sealing solution. Photos were taken using fluorescence microscope, and five visual fields were selected for each slice.

### Statistical analysis

Data are designated as the means  $\pm$  SD of three independent experiments. One-way ANOVA was performed to test the difference among the different groups. Each experiment was repeated at least three times with each data point done in duplicate. The binding data were analyzed by GraphPad Prism software.  $p < 0.05$  were considered to indicate a statistically significant difference.

### DATA AVAILABILITY

The data used to support the findings of this study are available from the corresponding author upon request.

## REFERENCES

- Anwanwan D, Singh SK, Singh S, Saikam V, Singh R. Challenges in liver cancer and possible treatment approaches. *Biochim Biophys Acta Rev Cancer*. 2020;1873:188314.
- Gonzalez-Castejon M, Visioli F, Rodriguez-Casado A. Diverse biological activities of dandelion. *Nutr Rev*. 2012;70:534–47.
- Saratale RG, Benelli G, Kumar G, Kim DS, Saratale GD. Bio-fabrication of silver nanoparticles using the leaf extract of an ancient herbal medicine, dandelion (*Taraxacum officinale*), evaluation of their antioxidant, anticancer potential, and antimicrobial activity against phytopathogens. *Environ Sci Pollut Res Int*. 2018;25:10392–406.
- Oh SM, Kim HR, Park YJ, Lee YH, Chung KH. Ethanolic extract of dandelion (*Taraxacum mongolicum*) induces estrogenic activity in MCF-7 cells and immature rats. *Chin J Nat Med*. 2015;13:808–14.
- Kisiel W, Barszcz B. Further sesquiterpenoids and phenolics from *Taraxacum officinale*. *Fitoterapia*. 2000;71:269–73.
- Ahmad VU, Yasmeen S, Ali Z, Khan MA, Choudhary MI, Akhtar F, et al. Taraxacin, a new guaianolide from *Taraxacum wallichii*. *J Nat Prod*. 2000;63:1010–1.
- Chen J, Wu W, Zhang M, Chen C. Taraxasterol suppresses inflammation in IL-1 $\beta$ -induced rheumatoid arthritis fibroblast-like synoviocytes and rheumatoid arthritis progression in mice. *Int Immunopharmacol*. 2019;70:274–83.
- Xu L, Yu Y, Sang R, Li J, Ge B, Zhang X. Protective effects of taraxasterol against ethanol-induced liver injury by regulating CYP2E1/Nrf2/HO-1 and NF- $\kappa$ B signaling pathways in mice. *Oxid Med Cell Longev*. 2018;2018:8284107.
- Muenst S, Laubli H, Soysal SD, Zippelius A, Tzankov A, Hoeller S. The immune system and cancer evasion strategies: therapeutic concepts. *J Intern Med*. 2016;279:541–62.
- Mizukoshi E, Kaneko S. Immune cell therapy for hepatocellular carcinoma. *J Hematol Oncol*. 2019;12:52.
- Sangro B, Sarobe P, Hervas-Stubbs S, Melero I. Advances in immunotherapy for hepatocellular carcinoma. *Nat Rev Gastroenterol Hepatol*. 2021;18:525–43.
- Cronin SJ, Penninger JM. From T-cell activation signals to signaling control of anti-cancer immunity. *Immunological Rev*. 2007;220:151–68.
- Bi Q, Liu Y, Yuan T, Wang H, Li B, Jiang Y, et al. Predicted CD4(+) T cell infiltration levels could indicate better overall survival in sarcoma patients. *J Int Med Res*. 2021;49:300060520981539.
- Xu G, Yuan G, Lu X, An L, Sheng Y, Du P. Study on the effect of regulation of *Cordyceps militaris* polypeptide on the immune function of mice based on a transcription factor regulatory network. *Food Funct*. 2020;11:6066–77.
- Jin X, Ruiz Beguerie J, Sze DM, Chan GC. *Ganoderma lucidum* (Reishi mushroom) for cancer treatment. *Cochrane Database Syst Rev*. 2016;4:CD007731.
- McCann SD, Kennedy JM, Tweet MS, Bryant SM. Sodium nitrite ingestion: an emerging trend in suicide attempts shared via online communities. *J Emerg Med*. 2021;60:409–12.
- Bruix J, Sherman M, Practice Guidelines Committee AASLD. Management of hepatocellular carcinoma. *Hepatology*. 2005;42:1208–36.
- Zhu H, Zhao H, Zhang L, Xu J, Zhu C, Zhao H, et al. Dandelion root extract suppressed gastric cancer cells proliferation and migration through targeting lncRNA-CCAT1. *Biomed Pharmacother*. 2017;93:1010–7.
- Ovadje P, Ammar S, Guerrero JA, Arnason JT, Pandey S. Dandelion root extract affects colorectal cancer proliferation and survival through the activation of multiple death signalling pathways. *Oncotarget*. 2016;7:73080–100.
- Ren F, Wu K, Yang Y, Wang Y, Li J. Dandelion polysaccharide exerts anti-angiogenesis effect on hepatocellular carcinoma by regulating VEGF/HIF-1 $\alpha$  expression. *Front Pharm*. 2020;11:460.
- Ghadir M, Khamseh ME, Panahi-Shamsabad M, Ghorbani M, Akbari H, Mehrjardi AZ, et al. Cell proliferation, apoptosis, and angiogenesis in non-functional pituitary adenoma: association with tumor invasiveness. *Endocrine*. 2020;69:596–603.
- Miao X, Xiang Y, Mao W, Chen Y, Li Q, Fan B. TRIM27 promotes IL-6-induced proliferation and inflammation factor production by activating STAT3 signaling in HaCaT cells. *Am J Physiol Cell Physiol*. 2020;318:C272–81.
- Jurikova M, Danihel L, Polak S, Varga I. Ki67, PCNA, and MCM proteins: markers of proliferation in the diagnosis of breast cancer. *Acta Histochem*. 2016;118:544–52.
- Couri T, Pillai A. Goals and targets for personalized therapy for HCC. *Hepatol Int*. 2019;13:125–37.
- Gonzalez H, Hagerling C, Werb Z. Roles of the immune system in cancer: from tumor initiation to metastatic progression. *Genes Dev*. 2018;32:1267–84.
- Dieu-Nosjean MC, Giraldo NA, Kaplon H, Germain C, Fridman WH, Sautes-Fridman C. Tertiary lymphoid structures, drivers of the anti-tumor responses in human cancers. *Immunological Rev*. 2016;271:260–75.
- Reid-Adam J, Yang N, Song Y, Cravedi P, Li XM, Heeger P. Immunosuppressive effects of the traditional Chinese herb Qu Mai on human alloreactive T cells. *Am J Transpl*. 2013;13:1159–67.
- Yang Y, Sun M, Yao W, Wang F, Li X, Wang W, et al. Compound kushen injection relieves tumor-associated macrophage-mediated immunosuppression through TNFR1 and sensitizes hepatocellular carcinoma to sorafenib. *J Immunother Cancer*. 2020;8:e000317.
- Zheng X, Jin W, Wang S, Ding H. Progression on the roles and mechanisms of tumor-infiltrating T lymphocytes in patients with hepatocellular carcinoma. *Front Immunol*. 2021;12:729705.
- Kim HD, Song GW, Park S, Jung MK, Kim MH, Kang HJ, et al. Association between expression level of PD1 by tumor-infiltrating CD8(+) T cells and features of hepatocellular carcinoma. *Gastroenterology*. 2018;155:1936–50 e1917.
- Xie Y, Xie F, Zhang L, Zhou X, Huang J, Wang F, et al. Targeted anti-tumor immunotherapy using tumor infiltrating cells. *Adv Sci*. 2021;8:e2101672.
- Zhang X, Xiong H, Liu L. Effects of taraxasterol on inflammatory responses in lipopolysaccharide-induced RAW 264.7 macrophages. *J Ethnopharmacol*. 2012;141:206–11.

## ACKNOWLEDGEMENTS

This work was supported by the Major Science and Technology Project of Xinxiang City (ZD2020005); Xinxiang Programs for Science and Technology Development (GG2019005); Henan Provincial Medical Science and Technology Research Project (SB201901064t).

## AUTHOR CONTRIBUTIONS

FR, HJ, and TZ conceived, designed, coordinate and directed this experiment. YZ, YQ, JS, YW, PW, and JG carried out the experiments. TZ drafted the primary version of manuscript. FR and TZ adjusted the main structure of the manuscript and revised the final draft. All authors read and approved the final manuscript. The decision of submitting the manuscript for publication was made by all authors.

## COMPETING INTERESTS

The authors declare no competing interests.

## ADDITIONAL INFORMATION

**Supplementary information** The online version contains supplementary material available at <https://doi.org/10.1038/s41420-022-01059-5>.

**Correspondence** and requests for materials should be addressed to Huijie Jia or Tiesuo Zhao.

**Reprints and permission information** is available at <http://www.nature.com/reprints>

**Publisher's note** Springer Nature remains neutral with regard to jurisdictional claims in published maps and institutional affiliations.



**Open Access** This article is licensed under a Creative Commons Attribution 4.0 International License, which permits use, sharing, adaptation, distribution and reproduction in any medium or format, as long as you give appropriate credit to the original author(s) and the source, provide a link to the Creative Commons license, and indicate if changes were made. The images or other third party material in this article are included in the article's Creative Commons license, unless indicated otherwise in a credit line to the material. If material is not included in the article's Creative Commons license and your intended use is not permitted by statutory regulation or exceeds the permitted use, you will need to obtain permission directly from the copyright holder. To view a copy of this license, visit <http://creativecommons.org/licenses/by/4.0/>.

© The Author(s) 2022